Materials and Design 96 (2016) 64–67

Contents lists available at ScienceDirect

Materials and Design

journal homepage: www.elsevier.com/locate/matdes

Tuning plasmon resonance in depth-variant plasmonic nanostructures

Xiaoxiao Jiang [a], Eunice Sok Ping Leong [b], Yan Jun Liu [b,*], Guangyuan Si [a]

[a] College of Information Science and Engineering, Northeastern University, Shenyang 110004, China
[b] Institute of Materials Research and Engineering, Agency for Science, Technology and Research (A*STAR), 2 Fusionopolis Way, #08-03, Innovis, Singapore 138634, Singapore

ARTICLE INFO

Article history:
Received 2 November 2015
Received in revised form 2 February 2016
Accepted 3 February 2016
Available online 3 February 2016

Keywords:
Plasmonic
Tunable colors
Ion beam milling

ABSTRACT

We demonstrate coaxial-aperture-based plasmonic nanostructures for tunable plasmon resonances in optically thick metal films. Accurate control of etching depth is achieved via cross-section investigation under a scanning electron microscope. Colorful surfaces are observed with varying geometries. The approach developed in this work is potentially useful for optical devices design and development in nanophotonics and integrated optics, especially for imaging and display applications.

Plasmonic color filters have drawn considerable attention and wide interest most recently. Various structures including nanoholes [1], nanorings [2], nanorods [3], nanoslits [4], metal-insulator-metal strips [5], and nanogratings [6], have been experimentally used for color generation thus far. Moreover, actively tunable color filters [7, 8] have also been realized by employing liquid crystals. Plasmonic color filters have irreplaceable advantages over conventional ones based on colorant pigmentation since they are ultra-compact, antifading, and integratable. Therefore, they are of particular importance for the development of display and imaging applications in the visible range [9–18].

Coaxial apertures are a unique structure for single layer metamaterials in the visible range in combination with electro-optical materials [19, 20]. Coaxial apertures are highly symmetrical in the 2D plane and therefore they could be polarization insensitive. This independency is extremely desirable for designing elegant plasmonic color filters with both high efficiency and simple architectures. Compared with conventional geometries (cylindrical nanoholes, for instance), nanorings can support propagating plasmon modes and they can transmit energy up to 90% at certain wavelengths [21] by properly designing the structural parameters. More importantly, such apertures are also potentially useful for plasmon assisted sensing [22–24], waveguiding [25, 26], and Raman spectroscopy [27]. Furthermore, such coaxial apertures can be used to enhance the second harmonic generation when combined with nonlinear materials [28]. Here, we report on coaxial-aperture-based plasmonic nanostructures in optically thick metal films. By precisely controlling the etching depth of the coaxial apertures, we are able to achieve accurate control of plasmon resonances in the visible regime.

Metal films (both Ag and Au) with various thicknesses and an adhesion (5 nm Ti) layer were deposited on quartz substrates using electron beam evaporation (Edwards Auto 306 E-Beam Evaporator) at 4×10^{-7} mbar with a deposition rate of 0.07 nm/s. Afterwards, direct focused ion beam (FIB) milling was carried out to define different patterns with varying etching depths. A single-beam (only the ion source) setup (FIB 200, FEI Corporation) was used and the milling current was set to be 70 pA. More details regarding the FIB milling process can be found elsewhere [29, 30]. Note that several important parameters may affect the final etching results and fine adjustment is thus necessary during the milling process. Transmission measurement was carried out using CRAIC QDI 2010™ with a 75 W broadband light source (xenon lamp). The probe light beam was focused to have a detecting area of 7.1 × 7.1 μm [2] using a 36× objective lens combined with a variable aperture. The measured transmission was normalized with the light through a bare quartz substrate. Both optical spectra and the corresponding optical images were collected using the attached spectrometer and CCD camera, respectively.

Fig. 1a is the sketch showing the coaxial structure proposed in this study. Coaxial nanocavities are supported by a quartz substrate (the adhesion is not shown). Fig. 1b demonstrates three most important parameters of coaxial apertures: the etching depth (d), the inner radius (r_i) and the outer radius (r_o). Typical top- and side-view SEM images are shown in Fig. 1c and d, respectively. A clear coaxial aperture can be observed from the top-view. In addition, the border region of the apertures shows slightly brighter colors compared with other regions due to material redeposition and long-time milling. From the cross-sectional image, one can clearly see that the gap width of the cavity is nonuniform

* Corresponding author.
E-mail addresses: liuy@imre.a-star.edu.sg (Y.J. Liu), siguang0323@hotmail.com (G. Si).

http://dx.doi.org/10.1016/j.matdes.2016.02.005
0264-1275/

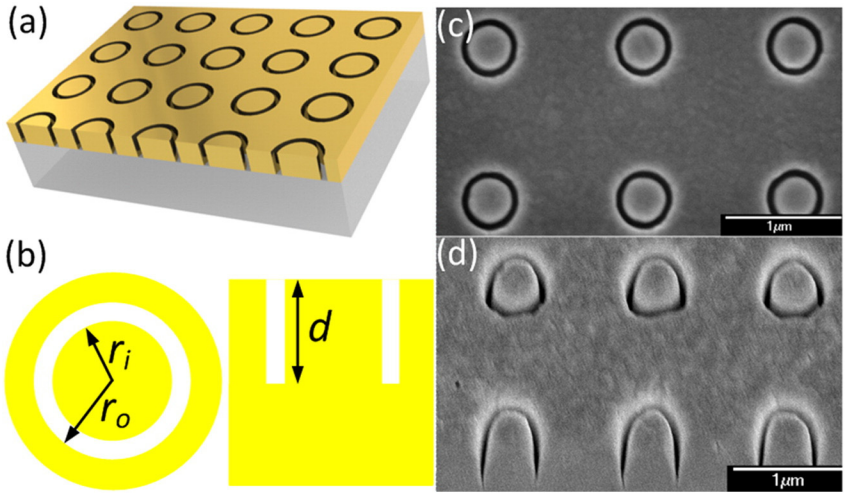

Fig. 1. (a) Schematic of gold coaxial apertures supported by a quartz substrate. (b) Top- and side-view sketches showing critical parameters for a coaxial aperture. (c) Top- and (d) side-view SEM images of coaxial apertures fabricated via FIB milling.

from top to bottom. In general, it decreases with increasing etching depth, giving rise to a tapered profile of the ring cavity.

It has been shown that coaxial apertures with varying gap widths are capable of filtering out individual colors from a broadband light source [2, 7]. Selective transmission can be obtained through the TE_{11} modes by engineering coaxial apertures with various geometrical designs [31, 32]. With the fixed thickness of a metal film, different combinations of diameters and gaps from the designed coaxial apertures can be used to generate various phase retardations in both transmission and reflection, hence affecting the propagation mode inside the cavities and leading to selected transmission/reflection of certain modes. In previous reports [33, 34], it was shown that two main types of surface plasmons in a coaxial aperture array can affect the transmission/reflection properties greatly: cylindrical surface plasmons (CSPs) and planar surface plasmons (PSPs). CSPs are highly dependent on the structural parameters. On the other hand, PSPs are mainly affected by the periodicity of the array. Finite difference time domain (FDTD) calculations were carried out (Lumerical, https://www.lumerical.com/). The dispersion model of metals is based on Johnson and Christy [35]. Fig. 2a shows the calculated transmission for coaxial aperture arrays with a fixed period of 1200 nm and different gap widths (r_o–r_i) from 40 nm to 120 nm in the step size of 40 nm. As can be seen, two apparent transmission peaks for each array are clearly observed. One peak strongly depends on the variation of the gap width, which is mainly attributed to the CSPs. The CSP peak redshifts with reducing gap widths. In contrast, the other one remains almost unaltered since the periodicity of the array is fixed to a constant (1200 nm in this case), which therefore results from PSPs. Using such a color-filtering working principle, different colors can be filtered out with various ring arrays, as shown in Fig. 2b. It is worth mentioning that the coaxial aperture arrays discussed here are milled through the metal film. The plasmon resonance effect can be well controlled by changing the gap width of the coaxial apertures and hence selective transmission can be obtained through the whole visible range using such aperture arrays with different gap widths.

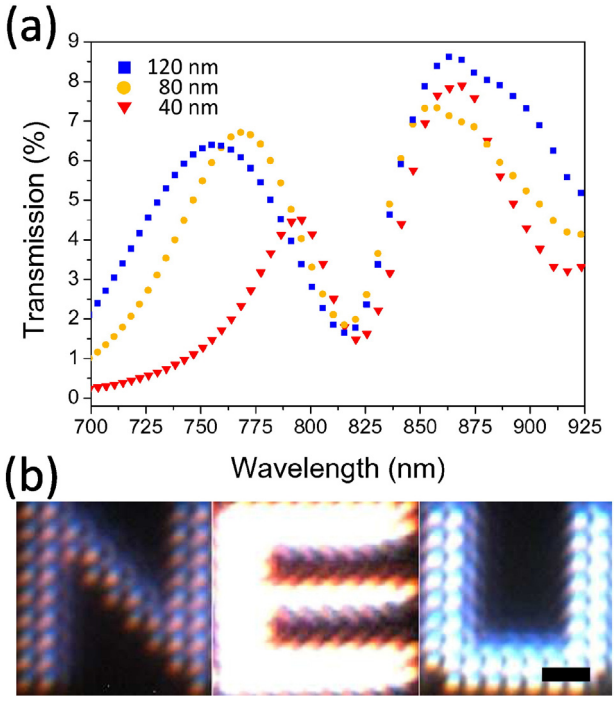

Fig. 2. (a) Calculated transmission for coaxial apertures with fixed period at 1200 nm and different gap widths (r_o–r_i) from 40 nm to 120 nm in increments of 40 nm with r_i fixed at 200 nm. (b) Optical image showing letters 'NEU' fabricated in a 140 nm gold film with 40 nm, 80 nm and 120 nm gap width for 'N', 'E' and 'U', respectively. The scale bar represents 2 μm.

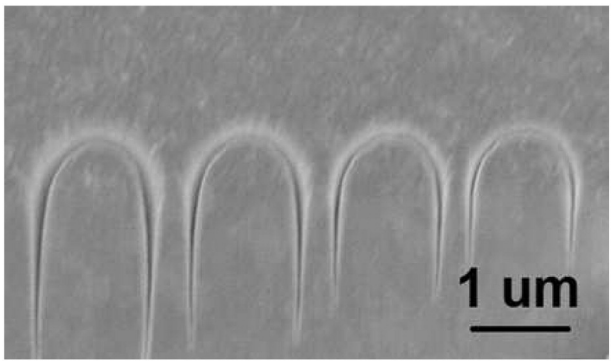

Fig. 3. SEM image showing fine adjustment on etching depth using FIB milling. Decreasing depth is shown from left (1600 nm) to right (700 nm) in the SEM image with the gap width of all four coaxial apertures set to 20 nm (r_o = 470 nm and r_i = 450 nm).

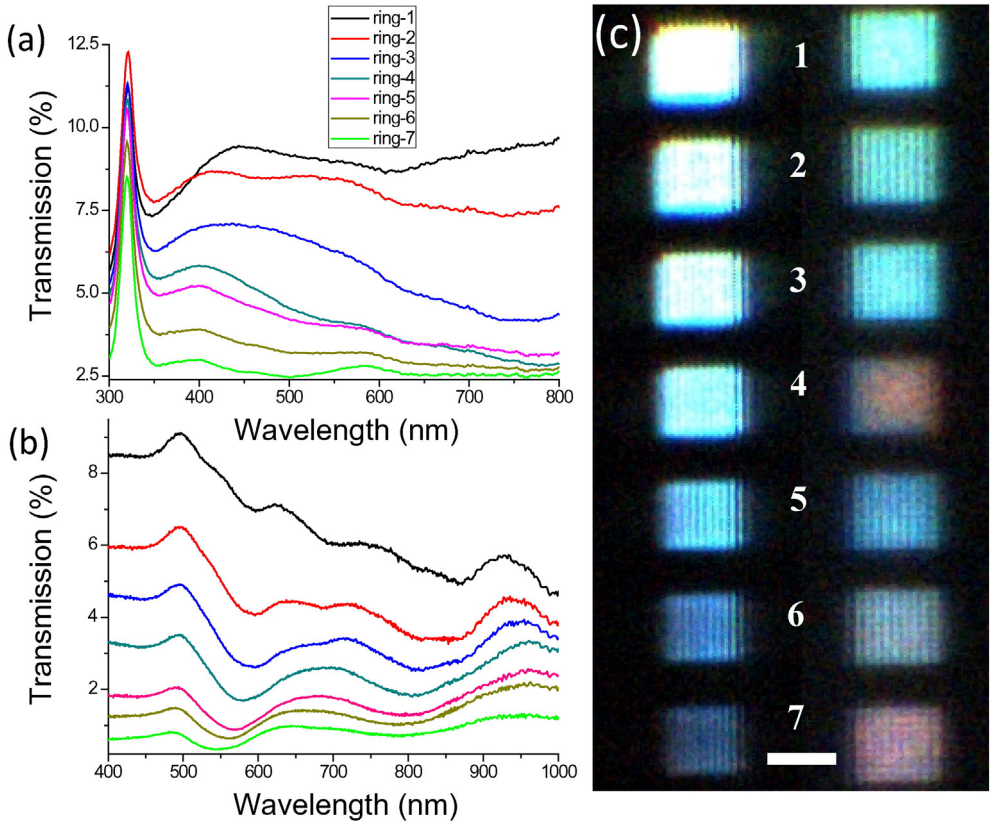

Fig. 4. Measured transmission for coaxial apertures with varying etching depths in a (a) 170 nm Ag film and (b) 170 nm Au film, respectively. (c) Transmission mode optical image of rings in the Ag (left column) and Au (right column) film. Scale bar, 5 μm.

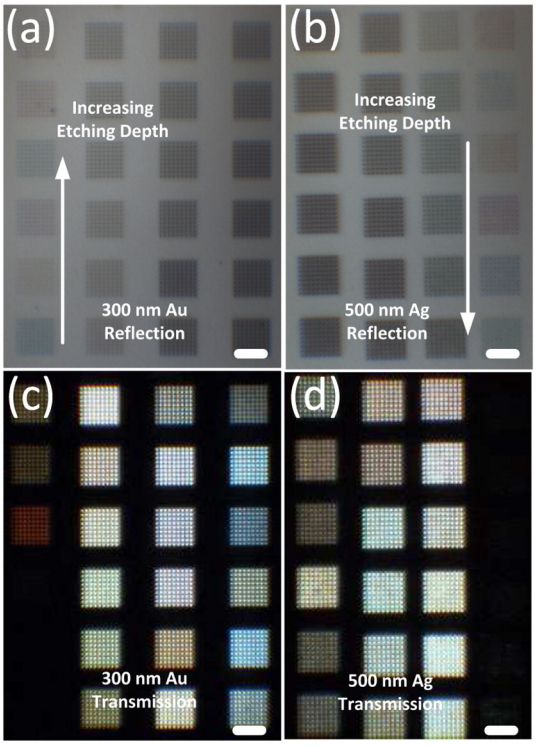

Fig. 5. Optical images for (a) 300 nm Au under reflection mode, (b) 500 nm Ag under reflection mode, (c) 300 nm Au under transmission mode, and (d) 500 nm Ag under transmission mode with varying etching depths of coaxial apertures. The gap width of all apertures are set to 30 nm ($r_o = 230$ nm and $r_i = 200$ nm). All scale bars are 5 μm.

On the other hand, adjusting the etching depth is another effective way to manipulate the plasmon resonance. Note that for non-etched-through coaxial apertures, they may become non-transparent, and therefore the transmission is not always measurable. However, different surfaces can be revealed under the reflection mode which will be discussed in detail in the following content. To precisely control the milling depth, several parameters need to be fine adjusted during the FIB lithography process. It is worth mentioning that the gap width at the top surface of an aperture is slightly larger than the set value for the milling process since the redeposition is almost inevitable and the ion beam induced damage is especially severe for deep etching. Nevertheless, one can accurately control the milling depth and obtain good sample surfaces (smooth) and sidewalls (nearly vertical) under optimized conditions. As shown in Fig. 3, gradually decreasing etching depths are demonstrated from left to right using the cross-sectioning function of the FIB system. The etch depth is from 1600 nm to 700 nm from left to right with 300 nm decrements. One can also clearly observe that the aperture width is increasing from bottom to top and very high aspect ratios (small gap widths and large etching depths) can be realized.

To investigate the effect with varying etching depths, we first fabricated coaxial apertures with 200 nm inner radius and 240 nm outer radius and 1200 nm array periodicity. The etching depth was varied from 170 nm (ring-1) to 110 nm (ring-7) in 10 nm step size in 170 nm thick Ag and Au films. The measured transmission spectra are plotted in Fig. 4a and b, respectively. The trend of increasing transmitted intensity with deeper etching is obvious. For the spectra of coaxial apertures in the Ag film (Fig. 4a), there are two resonance peaks observed when the etching depth is 110 nm, locating at ~400 nm and 580 nm, respectively. As the etching depth increases, the peak at 400 nm enhances considerably and redshifts gradually to about 450 nm for 170 nm etching

depth (milled through). On the other hand, the resonance peak at 580 nm barely shifts and rises for smaller etching depths (ring-7 to ring-4). Additionally, the two resonance peaks merge to form a broad peak (350 ~ 550 nm) for the curve of the 150 nm depth apertures (blue), which is due to the fabrication imperfections. Similar trends of resonance shift can be observed from the spectra of the apertures in the Au film (Fig. 4b). The peaks locate at 620 nm and 950 nm for the apertures with 110 nm depth. One should note that the average increments of transmitted energy are smoother and more uniform for the curves of apertures in Au than in Ag films since the milling rate for Au is much smaller than Ag under the same milling conditions and less ion-induced damage and fabrication imperfections are caused. The optical image of the rings in Ag/Au films under transmission mode is shown in Fig. 4c. Increasing intensity with larger etching depth is evident.

To further investigate the feasibility of color control under reflection mode, we increase the thickness of the metal film significantly to 300 nm (Au) and 500 nm (Ag) and expand the etching depth range accordingly. For the optical images in the reflection mode (Fig. 5a and b), one can see that colorful surfaces reveal for shallow etch. With increasing etching depths, the color turns to gray and finally black when the metal films are penetratingly milled. No transmission can be observed for shallow coaxial apertures since the film is opaque for both Au (left column in Fig. 5c) and Ag (right column in Fig. 5d). It is worth noting that the gap width also increased with larger etching depths (details can be found in Fig. 3) since the milling time was extended gradually.

In summary, we have presented precise control on plasmon resonances by accurately controlling the geometry of the coaxial apertures. As a result, colorful surfaces have been achieved in optically thick metal films. The approach shown in this work is potentially useful for imaging and display applications in novel nanophotonics devices.

Acknowledgements

This work was supported by the National Natural Science Foundation of China (Grant No. 61405031). E. S. P. Leong and Y. J. Liu acknowledge financial support from Agency for Science, Technology and Research (A*STAR) under the Grant No. 12302FG012.

References

[1] W.L. Barnes, A. Dereux, T.W. Ebbesen, Nature 424 (2003) 824.
[2] T. Alaridhee, A. Ndao, M.P. Bernal, E. Popov, A.L. Fehrembach, F.I. Baida, Opt. Express 23 (2015) 11687.
[3] V. Leitgeb, A. Trügler, S. Köstler, M.K. Krug, U. Hohenester, A. Hohenau, A. Leitner, J.R. Krenn, Nanoscale 8 (2016) 2974.
[4] E. Laux, C. Genet, T. Skauli, T.W. Ebbesen, Nat. Photonics 2 (2008) 161.
[5] W. Cai, U.K. Chettiar, H. Yuan, V.C. de Silva, A.V. Kildishev, V.P. Drachev, V.M. Shalaev, Opt. Express 17 (2009) 5925.
[6] B. Zeng, Y. Gao, F.J. Bartoli, Sci. Rep. 3 (2013) 2840.
[7] C. Park, Y. Yoon, V.R. Shrestha, C. Park, S. Lee, E. Kim, Opt. Express 21 (2013) 28783.
[8] D. Franklin, Y. Chen, A. Vazquez-Guardado, S. Modak, J. Boroumand, D. Xu, S.T. Wu, D. Chanda, Nat. Commun. 6 (2015) 7337.
[9] Y.J. Liu, G.Y. Si, E.S.P. Leong, B. Wang, A.J. Danner, X.C. Yuan, J.H. Teng, Appl. Phys. A Mater. Sci. Process. 107 (2012) 49.
[10] S. Yokogawa, S.P. Burgos, H.A. Atwater, Nano Lett. 12 (2012) 4349.
[11] T. Xu, Y.K. Wu, X. Luo, L.J. Guo, Nat. Commun. 1 (2010) 59.
[12] M.I. Benetou, J.S. Bouillard, P. Segovia, W. Dickson, B.C. Thomsen, P. Bayvel, A.V. Zayats, Nanotechnology 26 (2015) 444001.
[13] Y.S. Do, J.H. Park, B.Y. Hwang, S.M. Lee, B.K. Ju, K.C. Choi, Adv. Opt. Mater 1 (2013) 133.
[14] E.S.P. Leong, S. Wu, N. Zhang, W.W. Loh, E.H. Khoo, G.Y. Si, H.T. Dai, Y.J. Liu, Nanotechnology 25 (2014) 055203.
[15] L. Duempelmann, D. Casari, A. Luu-Dinh, B. Gallinet, L. Novotny, ACS Nano 9 (2015) 12383.
[16] K. Wang, Y. Chang, Y. Chen, C. Zhang, B. Wang, Mater. Des. 67 (2015) 159.
[17] C. Zhao, B. Zhang, S. Wang, P. Shang, S. Li, L. Yan, Mater. Des. 32 (2011) 947.
[18] Z. Li, S. Butun, K. Aydin, ACS Photonics 2 (2015) 183.
[19] E.H. Barakat, M.P. Bernal, F. Baida, Opt. Express 18 (2010) 6530.
[20] S.P. Burgos, R. de Waele, A. Polman, H.A. Atwater, Nat. Mater. 9 (2010) 407.
[21] Y. Poujet, J. Salvi, F.I. Baida, Opt. Lett. 32 (2007) 2942.
[22] A.E. Cetin, H. Altug, ACS Nano 6 (2012) 9989.
[23] P. Nordlander, ACS Nano 3 (2009) 488.
[24] E.M. Larsson, J. Alegret, M. Käll, D.S. Sutherland, Nano Lett. 7 (2007) 1256.
[25] P.B. Catrysse, S. Fan, Appl. Phys. Lett. 94 (2009) 231111.
[26] O. Kozina, I. Nefedov, L. Melnikov, A. Karilainen, Materials 4 (2011) 104.
[27] Z. Li, A.W. Clark, J.M. Cooper, Appl. Phys. Lett. 105 (2014) 033115.
[28] D. Lehr, J. Reinhold, I. Thiele, H. Hartung, K. Dietrich, C. Menzel, T. Pertsch, E.B. Kley, A. Tunnermann, Nano Lett. 15 (2015) 1025.
[29] X. Jiang, Q. Gu, F. Wang, J. Lv, Z. Ma, G. Si, Mater. Lett. 100 (2013) 192.
[30] G. Si, Y. Zhao, J. Lv, F. Wang, H. Liu, J. Teng, Y.J. Liu, Nanoscale 5 (2013) 4309.
[31] F.I. Baida, D. Van Labeke, Phys. Rev. B 67 (2003) 155314.
[32] F.I. Baida, A. Belkhir, D. Van Labeke, O. Lamrous, Phys. Rev. B 74 (2006) 205419.
[33] M.I. Haftel, C. Schlockermann, G. Blumberg, Appl. Phys. Lett. 88 (2006) 193104.
[34] M.I. Haftel, C. Schlockermann, G. Blumberg, Phys. Rev. B 74 (2006) 235405.
[35] P.B. Johnson, R.W. Christy, Phys. Rev. B 6 (1972) 4370.